Transmembrane Protein CMTM6 Alleviates Ocular Inflammatory Response and Improves Corneal Epithelial Barrier Function in Experimental Dry Eye

Yifan Zhou,[1,2] Baikai Ma,[1,2] Qiyao Liu,[3,4] Hongyu Duan,[1,2] Yangbo Huo,[3,4] Lu Zhao,[1,2] Jiawei Chen,[5] Wenling Han,[3,4] and Hong Qi[1,2,5]

[1]Department of Ophthalmology, Peking University Third Hospital, Beijing, China
[2]Beijing Key Laboratory of Restoration of Damaged Ocular Nerve, Peking University Third Hospital, Beijing, China
[3]Department of Immunology, Peking University Health Science Center, NHC Key Laboratory of Medical Immunology, Beijing, China
[4]Peking University Center for Human Disease Genomics, Beijing, China
[5]Institute of Medical Technology, Peking University Health Science Center, Beijing, China

Correspondence: Hong Qi, Department of Ophthalmology, Peking University Third Hospital, Beijing Key Laboratory of Restoration of Damaged Ocular Nerve, 49 North Garden Road, Haidian District, Beijing 100191, China; doctorqihong@163.com.
Wenling Han, Department of Immunology, Peking University Health Science Center, NHC Key Laboratory of Medical Immunology, Peking University Center for Human Disease Genomics, 38 Xueyuan Road, Haidian District, Beijing 100191, China; hanwl@bjmu.edu.cn.

Received: September 30, 2023
Accepted: December 4, 2023
Published: January 2, 2024

Citation: Zhou Y, Ma B, Liu Q, et al. Transmembrane protein CMTM6 alleviates ocular inflammatory response and improves corneal epithelial barrier function in experimental dry eye. *Invest Ophthalmol Vis Sci.* 2024;65(1):4. https://doi.org/10.1167/iovs.65.1.4

Purpose. To investigate the impact of transmembrane protein CMTM6 on the pathogenesis of dry eye disease (DED) and elucidate its potential mechanisms.

Methods. CMTM6 expression was confirmed by database analysis, real-time polymerase chain reaction (RT-PCR), western blot, and immunohistochemistry. Tear secretion was measured using the phenol red thread test. Immune cell infiltration was assessed through flow cytometry. Barrier function was evaluated by fluorescein sodium staining, immunofluorescence staining of zonula occludens 1 (ZO-1), and electric cell-substrate impedance sensing (ECIS) assessment. For silencing CMTM6 expression, siRNA and shRNA were employed, along with lentiviral vector-mediated overexpression of CMTM6. Proinflammatory cytokine levels were analyzed by RT-PCR and cytometric bead array (CBA) analysis.

Results. CMTM6 showed high expression in healthy human and mouse corneal and conjunctival epithelium but was notably reduced in DED. Notably, this downregulation was correlated with disease severity. *Cmtm6*$^{-/-}$ dry eye (DE) mice displayed reduced tear secretion, severe corneal epithelial defects, decreased conjunctival goblet cell density, and upregulated inflammatory response. Additionally, *Cmtm6*$^{-/-}$ DE mice and *CMTM6* knockdown human corneal epithelial cell-transformed (HCE-T) cells showed more severe barrier disruption and reduced expression of ZO-1. Knockdown of *CMTM6* in HCE-T cells increased inflammatory responses induced by hyperosmotic stress, which was significantly mitigated by *CMTM6* overexpression. Moreover, the level of phospho-p65 in hyperosmolarity-stimulated HCE-T cells increased after silencing *CMTM6*. Nuclear factor kappa B (NF-κB) p65 inhibition (JSH-23) reversed the excessive inflammatory responses caused by hyperosmolarity in *CMTM6* knockdown HCE-T cells.

Conclusions. The reduction in CMTM6 expression on the ocular surface contributes to the pathogenesis of DED. The CMTM6–NF-κB p65 signaling pathway may serve as a promising therapeutic target for DED.

Keywords: dry eye disease, CMTM6, corneal epithelium, inflammation, NF-κB, barrier disruption

Dry eye disease (DED) is a chronic inflammatory autoimmune disorder characterized by the disruption of homeostasis induced by desiccating stress and a vicious cycle of inflammation.[1,2] The worldwide incidence and prevalence of DED have been steadily increasing, resulting in a growing economic burden.[3–5] However, the underlying pathogenesis of DED remains poorly understood due to its multifactorial etiology. Additionally, the mainstay drugs for DED treatment have shown limited efficacy and a range of adverse events.[6–8] Therefore, it is essential to gain a deeper insight into the mechanisms underlying DED pathogenesis to improve treatment strategies.

Inflammation plays a pivotal role in DED.[9] Desiccating or hyperosmolar stress on the ocular surface triggers the activation of mitogen-activated protein kinases (MAPK) and nuclear factor kappa B (NF-κB) signaling pathways, leading to the production of proinflammatory cytokines, such as interleukin (IL)-1β, tumor necrosis factor alpha (TNF-α), and IL-6.[10–12] These cytokines, in turn, lead to corneal epithelial barrier dysfunction and goblet cell loss in the conjunctiva,

exacerbating the inflammatory response and creating a vicious self-perpetuating cycle, which ultimately reduces tear production and worsens symptoms.[11,13,14] The corneal and conjunctival epithelia act as the first line of defense against microbial agents and environmental insults.[15] In addition to serving as a physical barrier—for example, via the tight junction protein zonula occludens (ZO-1) in the cornea that maintains the paracellular barrier[16]—epithelial cells assume a significant role in the initiation and regulation of inflammatory responses. The corneal epithelium constitutively expresses a variety of negative immunomodulatory molecules, including pigment epithelial-derived factor (PEDF), netrin-1 (NTN-1), and thrombospondin-1 (TSP-1),[17–19] participates in the modulation of immune responses and prevention of excessive inflammation, which can potentially damage the cornea. Meanwhile, evidence suggests the involvement of epithelial cells in the innate immune response, as well as their playing a key role in linking innate and adaptive immunity.[20] Taken together, identifying targets capable of mitigating the inflammatory response of epithelial cells or protecting the integrity of the epithelial barrier may help to mitigate consistent inflammation in DED.

The chemokine-like factor (CKLF)-like MARVEL transmembrane domain-containing member (CMTM) gene family in humans is comprised of nine members: *CKLF* and *CMTM1* to *CMTM8*.[21,22] The products encoded by the CMTM family play multiple roles in the immune and reproductive systems. They are associated with the prognosis of various cancers and can induce anti-tumor immune effects by nodulating the cell cycle and signaling pathways.[23] CMTM6, located on chromosome 3p22 and comprised of 183 amino acids, is a transmembrane protein with a MARVEL domain widely recognized for its crucial role in regulating transmembrane protein trafficking. In 2017, two studies revealed that CMTM6 is a novel regulator of programmed death ligand-1 (PD-L1) that stabilizes its expression on the cell surface.[24,25] In addition to its role in tumor regulation, recent research has found that CMTM6 is important in autoimmune diseases, as well. In patients with antiphospholipid syndrome (APS), elevated CMTM6 expression suggests its potential involvement in APS development.[26] Additionally, in anti-neutrophil cytoplasmic antibody (ANCA)–associated vasculitis (AAV), decreased CMTM6 expression has been linked to increased PD-L1 degradation in lysosomes, contributing to AAV progression.[27] However, there is limited knowledge regarding its role in inflammation, especially in DED.

During our preliminary assessment, we first examined the expression of CMTM6 in healthy control and DED patients. We observed that conjunctival epithelial cells (CECs) of patients with DED showed significantly downregulated CMTM6 expression compared to those of healthy controls, strongly suggesting the involvement of CMTM6 in the progression of DED. Given the immunomodulatory ability of CMTM6 and its downregulation in DED, further investigations are warranted to understand the effects of CMTM6 on inflammation mediated by epithelial cells. Therefore, in this research, we examined the expression of CMTM6 in corneal and conjunctival epithelial cells and revealed its role in the pathogenesis of DED using two experimental dry eye (DE) models: a mouse model exposed to desiccating stress under scopolamine treatment and a primary human corneal epithelial cell-transformed (HCE-T) model exposed to hyperosmolarity stress. To identify the underlying mechanism, we examined the signaling pathway through which CMTM6 exerts its effects and determined whether the inhibition of this signaling pathway influences the effects of CMTM6 on inflammation in DED.

Materials and Methods

Clinical Participants

The Peking University Third Hospital Medical Science Research Ethics Committee approved all procedures involving human subjects in accordance with the tenets of the Declaration of Helsinki (Approval Number: M2023395). All participants provided written informed consent.

Healthy volunteers (control group) and patients with DED (DED group) were recruited. DED diagnosis and severity grading followed the "Chinese expert consensus on the definition and classification of dry eye (2020)"[28] and the "Chinese expert consensus on the examination and diagnosis of dry eye (2020)."[29] Tear film breakup time (TBUT) was used as the primary indicator. Mild DED was defined as having a TBUT of 6 to 10 seconds, and moderate to severe DED was defined by a TBUT of $\leq$5 seconds. Exclusion criteria included the following: usage of topical or systemic medicinal treatments, excluding artificial tears, within 2 weeks prior to recruitment; prevailing ocular infections; autoimmune or inflammatory disorders such as Sjögren syndrome, rheumatoid arthritis, or diabetes; prior history of ocular ailments or surgical procedures; meibomian gland dysfunction exceeding grade 2; or ongoing contact lens utilization.

Conjunctival Impression Cytology

Conjunctival epithelial cells were collected using impression cytology as previously described.[30] A nitrocellulose membrane (size, 5 $\times$ 5 mm^2; EMD Millipore, Burlington, MA, USA) was prepared as a small semicircular paper sheet and sterilized with ethylene oxide. The acetate membrane was applied to the surface of the bulbar conjunctiva, gently pressed with a sterilized glass rod for 5 to 10 seconds, placed in the lysate, and stored at −80°C. RNA was subsequently extracted to detect *CMTM6* and *TNFA* using real-time polymerase chain reaction (RT-PCR).

Animal Models

Female C57BL/6J mice, 6 to 8 weeks old, were obtained from Beijing Vital River Laboratory Animal Technology Co. Ltd. (Beijing, China). *Cmtm6* knockout (KO; *Cmtm6*$^{-/-}$) mice (C57BL/6J background) were generated by the Shanghai Model Organisms Center, Inc. (Shanghai, China) using CRISPR/Cas9 technology. Targeting of the *Cmtm6* gene start codon site was achieved by homologous recombination with the Luciferase-2A-EGFP-WPRE-pA expression frame (Supplementary Fig. S1). The successful generation of *Cmtm6*$^{-/-}$ mice was validated using RT-PCR (the primers are listed in Supplementary Table S1) and immunohistochemistry (IHC) analysis.

For the DE mouse model, mice were housed in a desiccator with humidity levels maintained below 25% and subjected to continuous airflow for 24 hours. Scopolamine hydrobromide (1 mg/0.2 mL PBS; Shanghai Macklin Biochemical Co., Shanghai, China) was subcutaneously administered twice daily for 14 days. Normal control mice of similar age and sex were maintained under conditions

with a relative humidity range of 50% to 75%, and they did not receive any treatments.

All animal experiments adhered to the guidelines outlined in the ARVO Statement for the Use of Animals in Ophthalmic and Vision Research. The study protocol was approved by the Institutional Animal Care and Use Committee (IACUC) of Peking University Health Science Center (Beijing, China; BCJE0151).

Phenol Red Thread Test

Tear production was measured using the phenol red thread test. A phenol red cotton thread was gently placed in the inner canthus of each eye for 15 seconds. The length of wetting (red) on the thread was recorded in millimeters.

Corneal Fluorescein Staining

One microliter of 0.5% sodium fluorescein was gently administered to the cornea of the mouse. Corneal fluorescein staining (CFS) was observed under a slit-lamp microscope after a 3-minute blinking period. The scoring standards for CFS were aligned with those established in our prior investigation.[17]

Tear Collection

PBS solution (1.5 µL) containing 0.1% bovine serum albumin (BSA) was dropped into the conjunctival sac.[31] Tear fluid was collected from the outer corner of the eye using a glass capillary tube of 1-µL capacity. The collected tear fluid was stored at −80°C.

Bone Marrow Adoptive Transfer

From the femur and tibia of wild-type (WT) mice, bone marrow cells were isolated. A quantity of 2×10^6 cells suspended in 200 µL of PBS was administered intravenously to 8-week-old recipient WT and KO mice that had been subjected to prior irradiation (9 Gy). After 8 weeks following the cell transfer, the recipient mice were used to develop DE.

Immunofluorescence Staining

Following euthanasia of the mice with CO_2, the eyes of the mice were extracted and embedded in an optimal cutting temperature compound. Cryostat sections were prepared. For immunofluorescence staining of wholemount corneal tissues, corneas were fixed in 4% paraformaldehyde for 10 minutes, followed by fixation in acetone for 3 minutes. The tissues were then subjected to a 1-hour blocking step using goat serum (SL038; Solarbio, Beijing, China) and incubated overnight at 4°C with anti–ZO-1 antibody (1:100, ab216880; Abcam, Cambridge, UK). After washing, the tissues were incubated for 1 hour with goat anti-rabbit IgG antibody (1:100, E-AB-1053; Elabscience, Wuhan, China). The quantitative analysis was conducted using ImageJ (National Institutes of Health, Bethesda, MD, USA) by measuring the immunofluorescence length of ZO-1.

Periodic Acid–Schiff Staining

The complete eyeball, inclusive of the eyelid, was excised and subsequently fixed in 4% paraformaldehyde at room temperature for 24 hours, following which paraffin embedding was performed. Sections underwent deparaffinization and were stained using periodic acid and Schiff's solution (PAS). Goblet cells with positive staining were quantified, and measurement of the span between the initial and final goblet cells was conducted.[32] Mean positive cell counts per millimeter were used to summarize the data collected.

IHC Analysis

The specimens underwent fixation, embedding, and sectioning as outlined earlier. After the blocking step, the samples were incubated overnight either with or without primary antibodies against CMTM6 (90329S; Cell Signaling Technology, Danvers, MA, USA), then for 1 hour with horseradish peroxidase–conjugated secondary antibodies. Color development was achieved using diaminobenzidine and hematoxylin. Cells exhibiting yellow or brown granules were regarded as positively stained.

Cell Culture and Development of the Hyperosmolar Stress Model

The HCE-T cell line was obtained from the Meisen Chinese Tissue Culture Collections (Meisen CTCC, Zhejiang, China). Short tandem repeat (STR) profiling performed by Suzhou Genetic Testing Biotechnology (Suzhou, China) was used to verify the cell line. HCE-T cells were cultivated in Gibco Dulbecco's Modified Eagle Medium/Nutrient Mixture F-12 (DMEM/F-12) medium (Thermo Fisher Scientific, Waltham, MA, USA) supplemented with 10 ng/mL human epidermal growth factor (hEGF), 5 µg/mL insulin, and 10% fetal bovine serum (Thermo Fisher Scientific). The cells were sustained at 37°C within a 5% CO_2 atmosphere.

HCE-T cells were exposed to a hypertonic environment (500 mOsM) for various durations. *CMTM6* mRNA expression was assessed at 3, 8, and 12 hours, and protein expression was examined after 24 hours. For gene expression analysis, cells were treated for 12 hours, and RNA was extracted. Western blot analysis was performed on cells treated for 24 or 36 hours, and the supernatant was used for cytometric bead array (CBA) analysis.

JSH-23 (HY-13982; Medchem Express, Monmouth Junction, NJ, USA) was used as an inhibitor of NF-κB p65; 50 µM JSH-23 was added to the cell culture medium, followed by incubation with 500 mOsM media for 8 or 24 hours. Dimethyl sulfoxide (DMSO) was used as a control.

Real-Time Polymerase Chain Reaction

RT-PCR was performed as previously reported.[33] All mRNA levels were normalized using β-actin. The $\Delta\Delta C_t$ method was used to assess the relative gene expression change. The primers employed are listed in Supplementary Table S1.

Western Blot Analysis

Protein lysates were prepared according to previously published methods.[34] The protein concentration was quantified using a BCA Protein Assay Kit (P0012S; Beyotime, Jiangsu, China). Western blot procedures were carried out following protocols as described previously.[35] Primary antibodies against the following proteins were used at a 1:1000 dilution: CMTM6 (90329S; Cell Signaling Technology), ZO-1

(ab216880; Abcam), p38 MAPK (8690S; Cell Signaling Technology), phospho-p38 MAPK (4511S, CST), Erk1/2 (4695S, CST), phospho-Erk1/2 (4370S), NF-κB p65 (8242S; Cell Signaling Technology), phospho-NF-κB p65 (3033S; Cell Signaling Technology), and β-actin (ab8226; Abcam).

Flow Cytometry

On day 14 of DE, bilateral draining lymph nodes (DLNs) were taken from each mouse and prepared as single-cell suspensions. Single-cell suspensions of DLNs were stimulated with RPMI culture medium containing brefeldin A (420601; BioLegend, San Diego, CA, USA) and Cell Activation Cocktail (423302; BioLegend) for 5 hours. Fluorescence-activated cell sorting (FACS) analysis (Canto II; Becton Dickinson, Franklin Lakes, NJ, USA) was performed using the following specific antibodies: Zombie Aqua Fixable Viability Kit (423101; BioLegend), Alexa Fluor 700 anti-mouse CD45 Antibody (103128; BioLegend), APC/Cyanine7 anti-mouse CD3 Antibody (100221; BioLegend), PerCP anti-mouse CD4 Antibody (100431; BioLegend), PE/Cyanine7 anti-mouse IFN-γ Antibody (505826; BioLegend), APC anti-mouse IL-17A Antibody (506916; BioLegend), Brilliant Violet 605 anti-mouse CD25 Antibody (102036; BioLegend), and PE anti-mouse FOXP3 Antibody (126404; BioLegend).

RNA Interference

HCE-T cells were transfected for 24 hours with a scrambled siRNA (siNC) or CMTM6 siRNA (siRNA#1, siRNA#2) using Invitrogen Lipofectamine RNAiMAX Transfection Reagent (13778030; Thermo Fisher Scientific), as recommended by the manufacturer. The mRNA levels of inflammatory cytokines were assessed after 12 hours of exposure to hyperosmotic stimulation, whereas the protein levels were evaluated using CBA or western blot after 36 hours of stimulation. The CMTM6 siRNA sequence was designed and synthesized by GenePharma (Shanghai, China). The sequences are shown in Supplementary Table S2.

Plasmid Construction and Transfection

GenePharma (Shanghai, China) constructed the CMV-GFP-Puro-sh-CMTM6 lentiviral vectors to silence CMTM6 expression. A lentivirus expressing control shRNA (shNC) was used as a negative control. A TG006-CMTM6-IRES-EGFP lentiviral vector was used to overexpress CMTM6. The TG006 lentiviral vector was used as a negative control. The sequences for shCMTM6 #1 and shCMTM6 #2 are shown in Supplementary Table S3.

Transfection utilized jetPRIME (Polyplus Transfection, Illkirch-Graffenstaden, France) according to the manufacturer's instructions. Viral supernatant was gathered 48 and 72 hours post-transfection, filtered through a 0.45-µm filter, and introduced to HCE-T cells alongside polybrene (5 µg/mL, PB-1000; Hanbio Co., Ltd., Shanghai, China). Puromycin (2 µg/mL, ST551; Beyotime) was used to select stable clones for 2 weeks.

Cytometric Bead Array

The concentrations of TNF-α and IL-6 in the tears of mice and supernatants of HCE-T cells were detected using CBA analysis (740150 and 740124; BioLegend) according to the manufacturer's guidelines.

Barrier Function Assessments

The ECIS ZΘ electric cell-substrate impedance sensing system (Applied Biophysics, Troy, NY, USA) was used to evaluate the integrity of the cellular barrier. The eight-well plate electrode arrays (8W1E; Applied Biophysics) underwent pretreatment with 10 mM L-cysteine for 15 minutes, followed by a 30-minute gelatin coating. Electrode impedance values were stabilized to minimize drift. The experiment was divided into three groups: normal HCE-T cells, siNC HCE-T cells, and siCMTM6 HCE-T cells, with three subwells in each group. One hundred thousand cells were resuspended in 400 µL of medium and spread in each well. A range of frequencies (1000–64 kHz) was used for continuous monitoring, with measurements acquired approximately every 2 minutes. Rb, signifying cell–cell contact resistivity, was obtained using the ECIS software. Each experiment was conducted in triplicate.

Statistical Analysis

Each experiment was independently performed at least three times. In the case of fluorescein sodium scoring, the phenol red thread test, and conjunctival goblet cell count, "*n*" specifically refers to the left eye of each mouse to maintain consistency and reduce variability. Prism 8.0 (GraphPad, Boston, MA, USA) was used for statistical analysis. Unpaired Student's *t*-test and one-way ANOVA followed by Dunnett's or Tukey's multiple comparisons test were used to determine significant differences among the groups. Data are shown as the mean ± standard deviation (SD), and $P < 0.05$ was considered statistically significant.

Results

CMTM6 Is Expressed at a High Level in Corneal and Conjunctival Epithelium

We initially analyzed CMTM6 expression in the BioGPS database and discovered that *Cmtm6* is widely distributed and expressed in various organs and tissues of mice (Fig. 1A). Among these, *Cmtm6* exhibited high expression levels in the cornea. To gain a deeper understanding of its distribution among different cell types on the ocular surface, we analyzed adult human corneas and adjacent conjunctivas using a public dataset (GSE182583). As shown in Figure 1B, *CMTM6* was highly expressed in corneal and conjunctival epithelial cells. To validate this result by RT-PCR, we separately collected the corneal epithelium, corneal stroma, and conjunctiva from healthy mice. Our findings demonstrated significantly higher expression levels of *Cmtm6* in the corneal epithelium and conjunctiva compared to the corneal stroma (Fig. 1C), underscoring its potential significance in corneal and conjunctival epithelial biology. In line with these alterations in gene expression, immunohistochemical staining of the normal cornea (Fig. 1D) and conjunctiva (Fig. 1E) revealed that CMTM6 was highly expressed in the epithelium, with the stroma exhibiting less intense staining.

CMTM6 Is Significantly Decreased in Patients With DED and DE Models In Vivo and In Vitro

We compared CMTM6 expression of CECs taken from patients with DED and healthy individuals. We found a

Investigative Ophthalmology & Visual Science

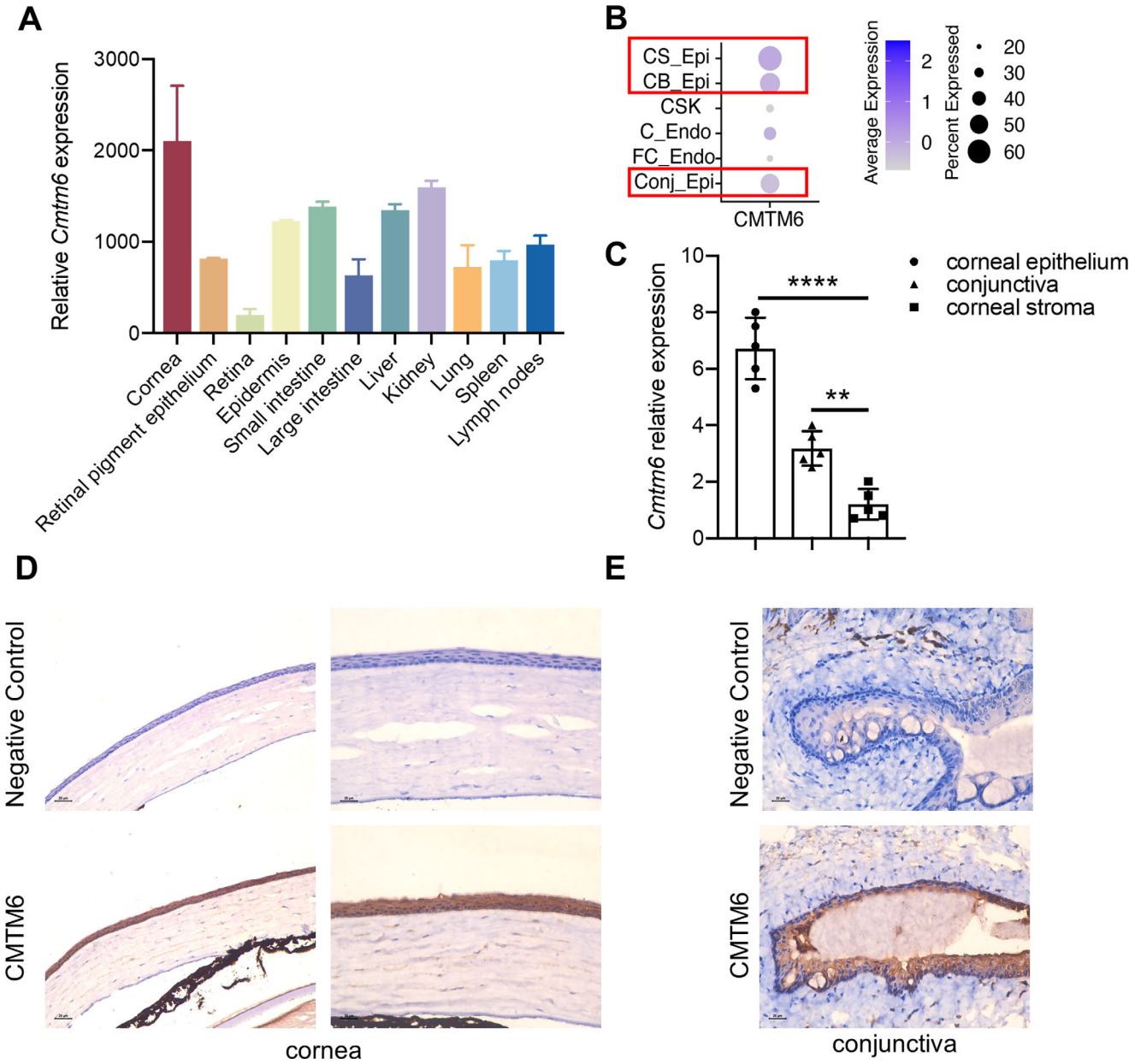

Figure 1. CMTM6 is expressed at a high level in corneal and conjunctival epithelium. (**A**) The tissue and organ distributions of *Cmtm6* were analyzed within the BioGPS database. (**B**) The detection of CMTM6 expression in adult human corneas and adjacent conjunctivas was carried out utilizing GSE182583 ($n = 4$). (**C**) The expression of *Cmtm6* in corneal epithelium, corneal stroma, and conjunctiva of healthy mice was assessed by RT-PCR ($n = 5$ in each group). (**D**, **E**) The protein level of CMTM6 was evaluated by IHC. Representative images of cornea (**D**) and conjunctiva (**E**) are shown. *Scale bars*: 20 µm. The results of a one-way ANOVA and Dunnett's multiple comparisons test are displayed as mean ± SD; "*n*" represents both eyes from a single mouse (**C**). $^{**}P < 0.01$, $^{****}P < 0.0001$. CS_Epi, corneal superficial epithelial cells; CB_Epi, corneal basal epithelial cells; CSKs, corneal stroma keratocytes; C_Endo, corneal endothelial cells; FC_Endo, fibroblastic corneal endothelial cells; Conj_Epi, conjunctival epithelial cells.

significant increase in *TNFA* mRNA levels in the CECs of patients with DED compared to healthy controls, whereas the expression of *CMTM6* was significantly decreased in the DED group (Figs. 2A, 2B). To further explore the relationship between CMTM6 and DED severity, especially corneal epithelial barrier disruption, patients with DED were categorized into two groups based on TBUT: mild DED ($n = 8$) and moderate to severe DED ($n = 26$). Patients with moderate to severe DED exhibited considerably decreased *CMTM6* expression in their CECs compared to those with mild DED (Fig. 2C), indicating the effects of DED on inflammation and barrier.

Next, we created a mouse model of DE to compare CMTM6 expression between DE and negative control (NC) mice. Consistent with the findings in patients, CMTM6 mRNA and protein levels were markedly decreased in the corneas of DE mice compared to those in NC mice (Figs. 2D, 2E). To further elucidate the changes in CMTM6 expression within corneal epithelial cells, we assessed CMTM6 mRNA and protein levels in HCE-T cells in response to a hyperosmotic

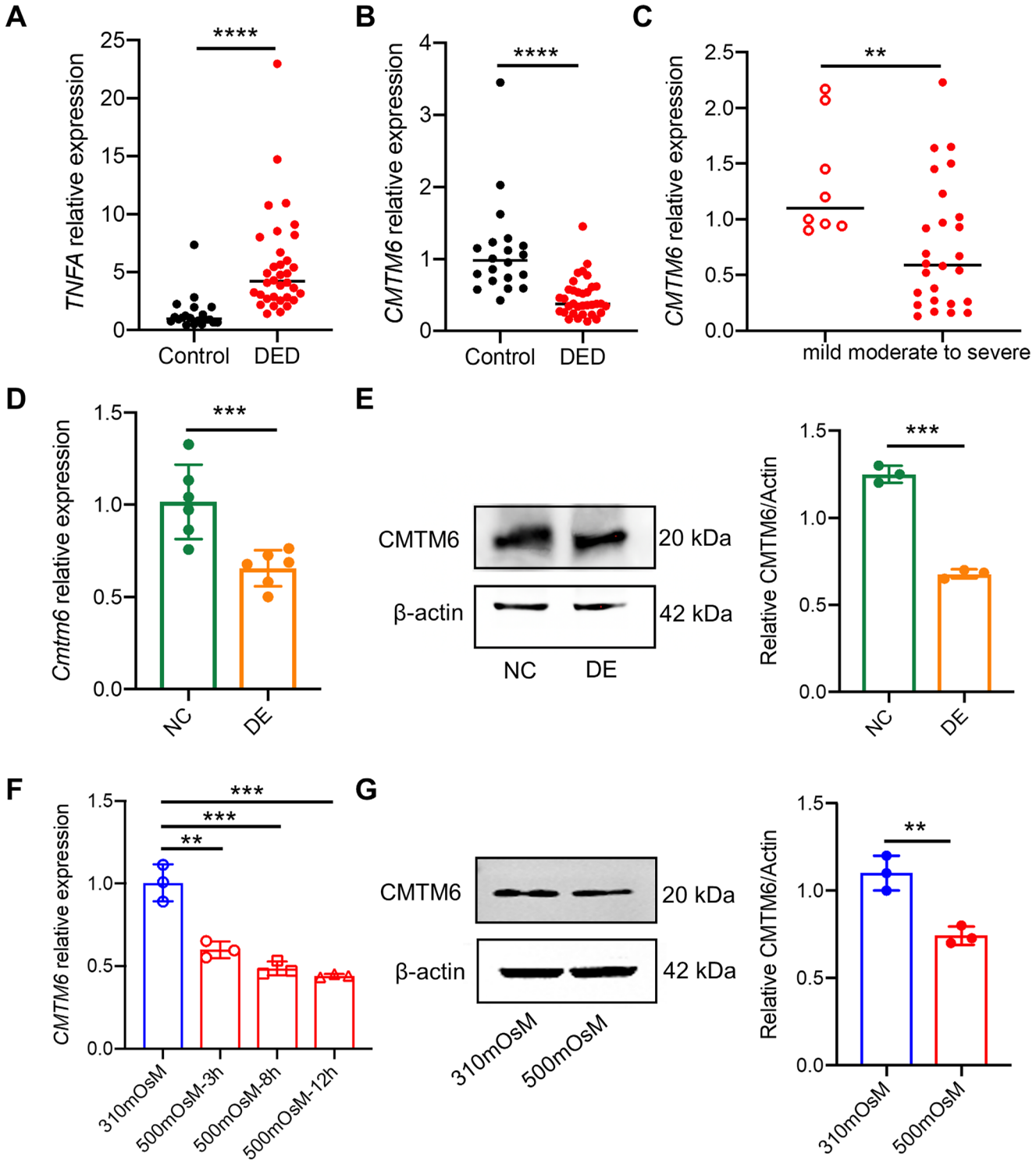

Figure 2. CMTM6 is significantly decreased in patients with DED and DE models in vivo and in vitro. (**A**, **B**) Conjunctival epithelial cells from patients with DED (n = 34) and healthy individuals (n = 20) were collected, and the expression of *Tnfa* (**A**) and *Cmtm6* (**B**) was detected. (**C**) Patients with DED were divided into two groups according to CFS scores: mild DED (n = 8) and moderate to severe DED (n = 26). The expression of *Cmtm6* was examined by RT-PCR. (**D**, **E**) A mouse model of DE was established using scopolamine hydrobromide injection. At day 14, all of the mice were sacrificed and corneas were collected (n = 6 in each group). (**D**) CMTM6 mRNA expression was detected by RT-PCR. (E) CMTM6 protein expression was measured by western blot analysis. (**F**, **G**) An in vitro DE model was established by culturing HCE-T cells in a hypertonic environment (500 mOsM). (**F**) *Cmtm6* mRNA expression levels were measured at 3, 8, and 12 hours following hyperosmotic stimulation. (**G**) CMTM6 protein expression level was measured at 24 hours. Results are shown as mean ± SD. Two-group statistical analysis was conducted using the unpaired Student's t-test (**A**–**E**, **G**). Four groups were compared using one-way ANOVA followed by Dunnett's multiple comparisons test (**F**); "n" represents both eyes from a single mouse (**D**, **E**). $^{**}P < 0.01$, $^{***}P < 0.001$, $^{****}P < 0.0001$.

Investigative Ophthalmology & Visual Science

medium at 500 mOsM. Figure 2F showed significant downregulation of *CMTM6* mRNA expression at 3, 8, and 12 hours following hyperosmotic stimulation of HCE-T cells, with the most pronounced decrease observed at 12 hours. After 24 hours of hyperosmotic stimulation, a marked reduction in CMTM6 protein levels was observed (Fig. 2G). Collectively, these findings indicate that CMTM6 is involved in the development of DED.

CMTM6 Alleviates Damage in DE Mice

For an in-depth exploration of the role of CMTM6 in DE pathogenesis, *Cmtm6*-knockout *(Cmtm6*$^{-/-}$) mice were generated. We initially used *Cmtm6*$^{-/-}$ mice to establish a DE model and examined green fluorescent protein (GFP) expression to further confirm the expression of CMTM6 in DE. Consistent with the results shown in Figure 2E, the corneal epithelium exhibited high levels of CMTM6 expression during normal ocular homeostasis. Conversely, a significant reduction in CMTM6 expression within the corneal epithelium was observed in the *Cmtm6*$^{-/-}$ mice with DE (Supplementary Fig. S2).

To further explore the contribution of decreased CMTM6 levels to DE, we assessed the function of CMTM6 in maintaining ocular surface homeostasis in WT and *Cmtm6*$^{-/-}$ mice under normal conditions. No significant differences were found in corneal fluorescein scores or tear production between the two groups (Figs. 3A, 3B). Furthermore, the density of conjunctival goblet cells was equally consistent in both WT and *Cmtm6*$^{-/-}$ mice, as shown by PAS staining (Fig. 3C). For deeper insights into the role of CMTM6 in DE, we exposed WT and *Cmtm6*$^{-/-}$ mice to desiccating stress conditions. Although the corneas of WT DE mice exhibited severe punctate epithelial defects, those of *Cmtm6*$^{-/-}$ DE mice showed more extensive injury, marked by notably higher fluorescein staining scores (Fig. 3D). Tear production in the *Cmtm6*$^{-/-}$ DE group was considerably lower compared to the WT DE group (Fig. 3E). Furthermore, *Cmtm6*$^{-/-}$ DE mice displayed a greater degree of loss and a lower density of conjunctival goblet cells (Fig. 3F).

Because $CD4^+$ T cells, particularly T helper 1 (Th1), Th17, and regulatory T cells (Tregs), play important roles in DED progression, we utilized flow cytometry to assess the percentages of these cells in the DLNs of the mice after 14 days of desiccation. The results showed that the percentage of Th1 and Th17 cells in the DLNs of *Cmtm6*$^{-/-}$ DE mice was significantly higher in contrast to that of WT DE mice, whereas the percentage of Tregs was not significantly different between the two groups (Fig. 4A). Furthermore, we examined the effects of CMTM6 on the production of proinflammatory cytokines in DE using RT-PCR and CBA. RT-PCR analysis revealed a notable elevation in the mRNA expression levels of the inflammatory cytokines *Tnfa*, *Il1b*, and *Il6* in the corneas of *Cmtm6*$^{-/-}$ DE mice compared to WT DE mice (Figs. 4B–4D). Moreover, Figure 4E shows an increase in the concentration of TNF-α in tears of *Cmtm6*$^{-/-}$ DE mice compared with WT DE mice.

Non-Hematopoietic Cell–Derived CMTM6 Suppresses Inflammation in DE Mice

Based on the finding that CMTM6 is highly expressed within the corneal and conjunctival epithelia and is downregulated in DE, we conducted bone marrow adoptive transfer experiments to elucidate the role of non-hematopoietic cell–derived CMTM6 in the pathogenesis of DE. Specifically, bone marrow grafts from WT mice were sequentially transplanted into irradiated WT mice (WT-WT) and *Cmtm6*$^{-/-}$ mice (WT-KO). Two months after marrow re-establishment, DE was induced (Supplementary Fig. S4A). As shown in Supplementary Figure S4B, the defect in the corneal epithelium was mild before DE induction. After 14 days of desiccation, the CFS scores were higher in WT-KO mice than in WT-WT mice. Moreover, compared with those in WT-WT mice, the levels of the proinflammatory factors *Tnfa*, *Il1b*, and *Il6* in the corneas of WT-KO mice were significantly increased (Supplementary Figs. S4C–S4E). These results indicate that non-hematopoietic cell–derived CMTM6 has a suppressive effect on inflammatory response in the DE mouse model.

CMTM6 Reduces Barrier Disruption In Vivo and In Vitro

The dysfunction of the corneal epithelial barrier assumes a central role in the pathogenesis of DED.[36] This disruption can arise as a consequence of inflammation or may induce and further exacerbate the inflammatory response.[37,38] We observed that the area of corneal epithelial defects, which represents the degree of barrier disruption, was increased in the *Cmtm6*$^{-/-}$ DE group compared with the WT DE group (Fig. 3D). As illustrated in Figure 5A, the corneal epithelium of WT and *Cmtm6*$^{-/-}$ mice under normal control conditions exhibited normal expression of ZO-1, with a well-organized and intricate reticular morphology. Conversely, in WT mice with DE, a notable reduction was observed in the abundance and integrity of ZO-1, accompanied by a disrupted morphology. Furthermore, the loss of ZO-1 and the disrupted morphology were significantly exacerbated in the corneal epithelium of *Cmtm6*$^{-/-}$ DE mice. These observations strongly suggest that CMTM6 exerts a protective effect on the epithelial barrier in vivo.

To further confirm the effect of CMTM6 on the epithelial barrier, we performed in vitro experiments using HCE-T cells. Changes in the barrier resistance of HCE-T cells under hyperosmotic stress were examined using ECIS. Resistance data at a frequency of 4000 Hz are shown in Supplementary Figure S5A for both normal cultured HCE-T cells and hyperosmotic-stimulated HCE-T cells. HCE-T cells grown in 310-mOsM media reached the stabilization resistance of ~13,000 Ω; however, HCE-T cells stimulated by 500 mOsM reached a plateau phase with a resistance of only ~6000 Ω. Supplementary Figure S5B shows that the endpoint resistance values of HCE-T cells at 310 mOsM were significantly higher than those at 500 mOsM. Moreover, to confirm whether the decrease in resistance in hyperosmotic cells was due to decreased barrier function, we analyzed the Rb parameters, which reflect the paracellular barrier strength, after the stabilization of resistance (i.e., when the plateau phase was reached). The results showed that the Rb values were lower in 500-mOsM media than in 310-mOsM media (Supplementary Fig. S5C). The endpoint Rb values also supported the reduction in barrier function that was observed (Supplementary Fig. S5D). We then monitored the effects of altered CMTM6 expression on barrier resistance. Using cells in which CMTM6 expression was reduced using siRNA, we detected significantly decreased resistance values compared to those in the siNC group (Figs. 5B, 5C). Moreover, *CMTM6* knockdown cells

Investigative Ophthalmology & Visual Science

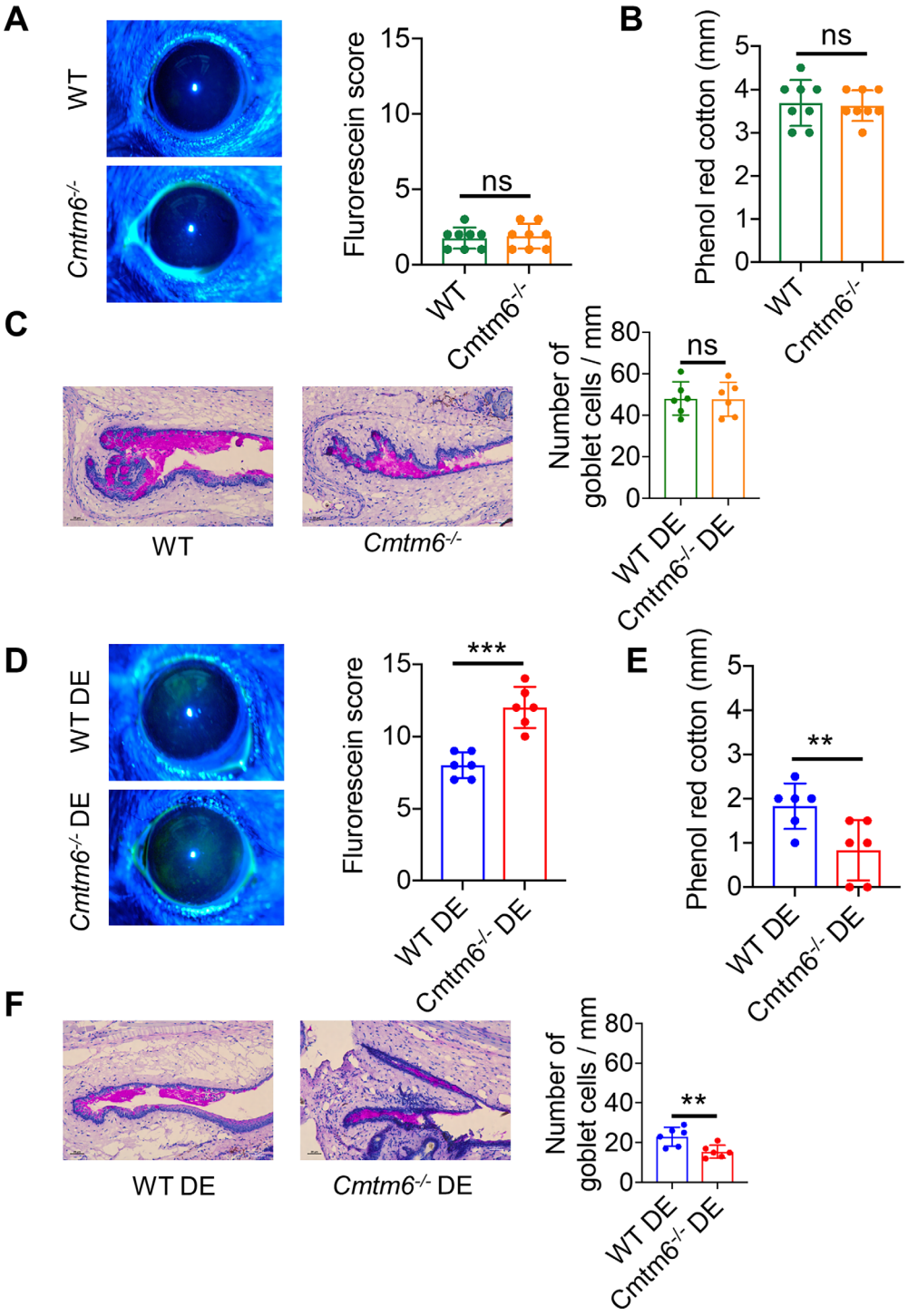

Figure 3. CMTM6 alleviates damage in DE mice. (**A**, **D**) CFS was used to evaluate corneal epithelial defects. (**B**, **E**) Tear production was examined using the phenol red thread test. (**C**, **F**) The conjunctival goblet cells were stained with PAS, and the positive cells were counted. *Scale bars*: 20 µm. Results are shown as mean ± SD (n = 6–8 in each group). A two-group statistical analysis was conducted using the unpaired Student's t-test; "n" represents one eye per mouse (**A**–**F**). $^{**}P < 0.01$, $^{***}P < 0.001$; ns, non-significant.

had significantly lower Rb values compared with those of control cells (Figs. 5D, 5E). In addition, after the knockdown of *CMTM6* in HCE-T cells using siRNA or shRNA, protein levels of ZO-1 were decreased compared with those in the control groups (Figs. 5F, 5G). These results demonstrate that CMTM6 preserves barrier function by regulating tight junction proteins.

CMTM6 Attenuates Inflammation Stimulated by Hyperosmolarity in HCE-T Cells

Previous studies, including ours, have demonstrated that the mRNA and protein levels of TNF-α, IL-1β, and IL-6 are significantly upregulated in HCE-T cells stimulated by hyperosmolarity. To confirm the role of CMTM6 in

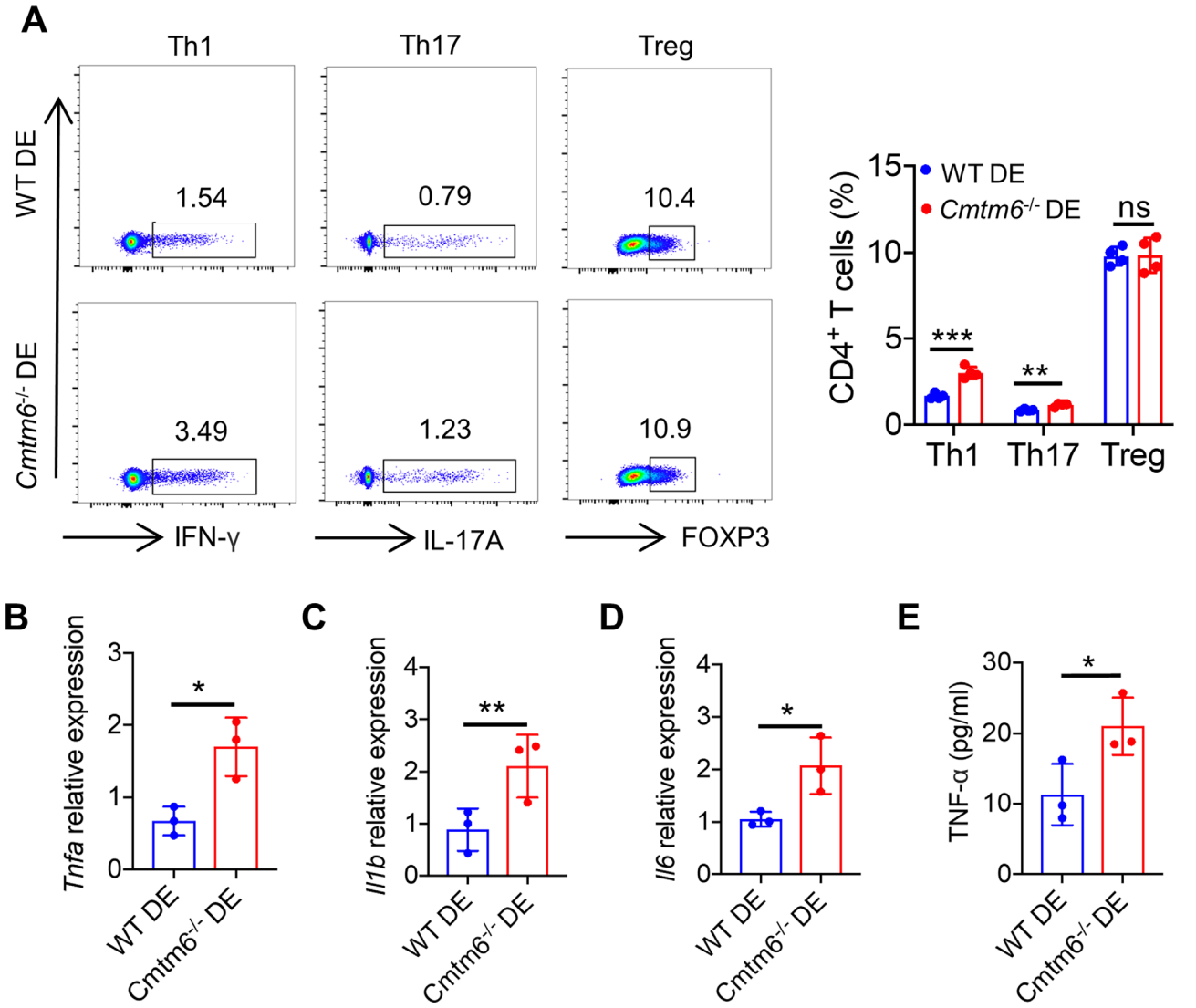

Figure 4. CMTM6 reduces DLNs Th1 and Th17 cell infiltration and proinflammatory cytokine production in DE mice. (**A**) Representative flow cytometry plots and quantitative summary of Th1, Th17, and Treg percentages among the DLNs. (**B–D**) RT-PCR was used to examine the production of proinflammatory cytokines *Tnfa* (**B**), *Il1b* (**C**), and *Il6* (**D**) in corneas. (**E**) The expression of TNF-α in tears was measured using CBA. Results are shown as mean ± SD (n = 3–4 in each group). A two-group statistical analysis was conducted using the unpaired Student's t-test; "n" represents bilateral draining lymph nodes (**A**) or both eyes (**B–E**) from a single mouse. *$P < 0.05$, **$P < 0.01$, ***$P < 0.001$.

mediating hyperosmolarity-induced inflammation, we employed a lentiviral system to establish stable overexpression of *CMTM6* in HCE-T cells, which was verified through RT-PCR and western blot analyses (Figs. 6A, 6B). As shown in Figures 6C–6E, the mRNA levels of *TNFA*, *IL1B*, and *IL6* were decreased in CMTM6-overexpressing HCE-T cells compared with control cells. Moreover, the protein level of IL-6 was downregulated in CMTM6-overexpressing HCE-T cells (Fig. 6F).

Next, siRNA was used to knockdown the expression of *CMTM6*. CMTM6 siRNA silencing significantly reduced both mRNA and protein levels in HCE-T cells compared to siNC pretreatment (Supplementary Figs. S6A–6B). Expression of *TNFA*, *IL1B*, and *IL6* mRNA was higher in the *CMTM6* siRNA group than in siNC groups (Supplementary Figs. S6C–S6E). Consistent with the RT-PCR results, the knockdown of CMTM6 upregulated the protein level of IL-6 (Supplementary Fig. S6F). To further silence CMTM6 in a stable manner, HCE-T cells were transduced with lentivirus expressing either a control shRNA or a CMTM6-specific shRNA (Figs. 7A, 7B). RT-PCR revealed that CMTM6 silencing significantly increased the expression of *TNFA*, *IL1B*, and *IL6* (Figs. 7C–7E). Meanwhile, the concentration of IL-6 in the supernatant was elevated in CMTM6-silenced cells at 500 mOsM (Fig. 7F). These results demonstrate that CMTM6 attenuates the inflammatory response in hyperosmolarity-stimulated HCE-T cells.

CMTM6 Suppresses Inflammation Through the NF-κB/p65 Pathway in HCE-T Cells Under Hyperosmotic Stress

Next, we determined how CMTM6 affects inflammatory response. The MAPK and NF-κB pathways have been reported to be activated during inflammation in DED. We

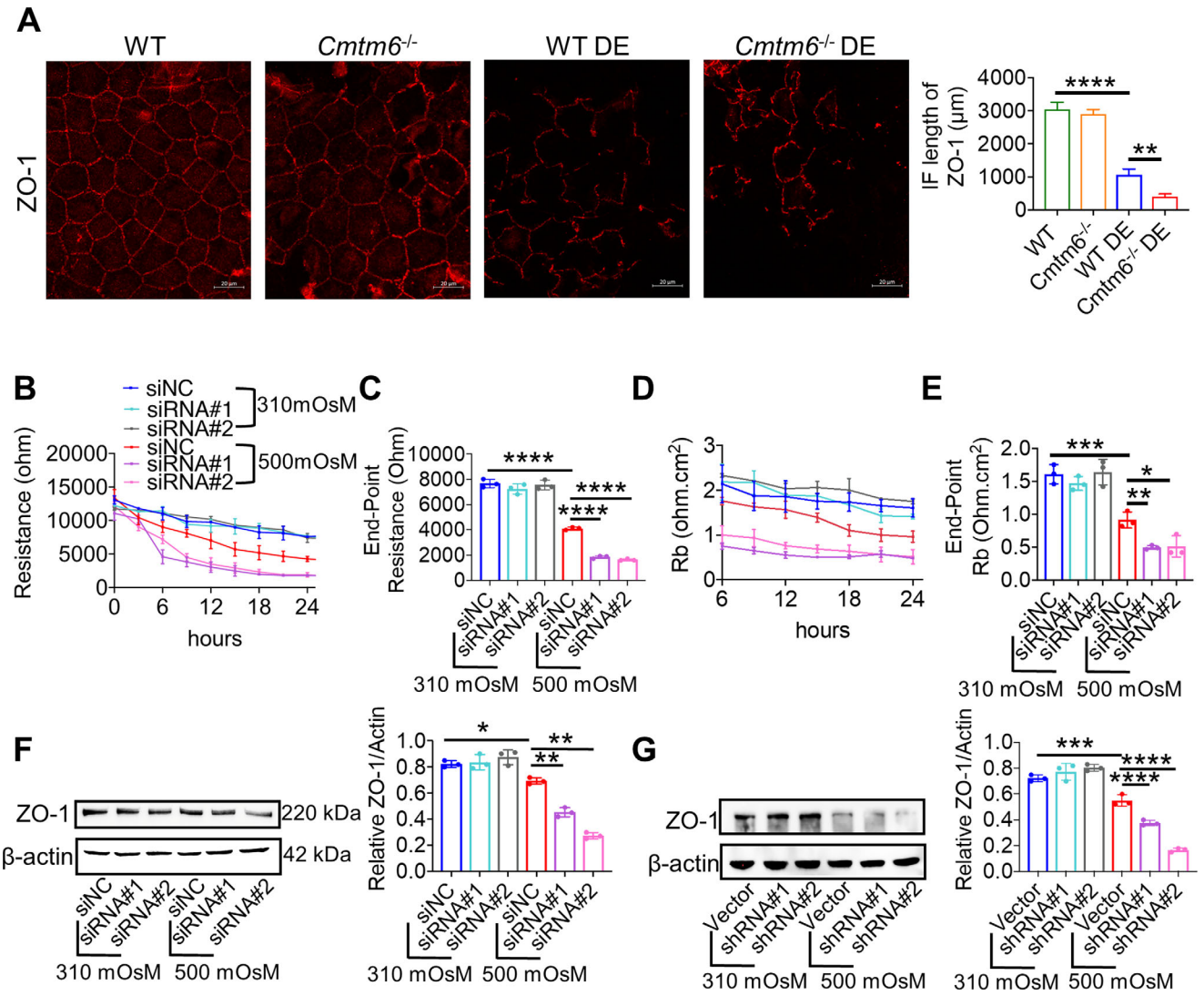

Figure 5. CMTM6 reduces barrier disruption in vivo and in vitro. (**A**) Immunofluorescence analysis of ZO-1 in wholemount corneal tissues with quantification by ImageJ. *Scale bars*: 20 µm. (**B**–**E**) Changes in the barrier resistance of HCE-T cells were examined using ECIS. (**B**) Resistance measurements generated at 4000 Hz from HCE-T cells grown in 310- and 500-mOsM culture media. (**C**) The endpoint resistance values of HCE-T cells. (**D**) Rb parameters were measured to reflect the paracellular barrier strength after the stabilization of resistance. (**E**) The endpoint Rb values of HCE-T cells. (**F**, **G**) After *Cmtm6* knockdown in HCE-T cells using siRNA (**F**) or shRNA (**G**), protein levels of ZO-1 were detected using western blot analysis. Results are shown as mean ± SD. Four groups were compared using one-way ANOVA followed by Tukey's multiple comparisons test (**C**, **E**–**G**). *$P < 0.05$, **$P < 0.01$, ***$P < 0.001$, ****$P < 0.0001$.

detected the activation of extracellular signal–related kinases (Erks), p38, and p65 in HCE-T cells. The results showed that, compared to the 310-mOsM group, the 500-mOsM group had higher levels of phospho-Erk (p-Erk), phospho-p38 (p-p38), and phospho-p65 (p-p65). However, the expression of p-p65 was further increased in *CMTM6*-silenced HCE-T cells treated with 500 mOsM (Fig. 8B), whereas no significant differences were observed in the expression of p-Erk and p-p38 (Fig. 8A). Next, we used the p65 inhibitor JSH-23 to examine the possibility of p65 participation in the inflammatory response induced by CMTM6; the effect of JSH-23 was measured using western blot analysis (Fig. 8C). Inhibition of p65 significantly rescued the upregulation of *TNFA*, *IL1B*, and IL-6 observed in *CMTM6*-silenced HCE-T cells at 500 mOsM (Figs. 8D–8G). Therefore, we suggest that CMTM6 reduces inflammation by inhibiting NF-κB/p65 activation.

Discussion

Elevated tear osmolarity serves as the initiating factor in the development of DED, leading to increased expression of proinflammatory cytokines, such as TNFα, IL-1β, and IL-6. These cytokines initiate an inflammatory cascade that results in sustained damage to the ocular surface.[9,39] Therefore, identifying targets capable of inhibiting the inflammatory response and understanding the underlying mechanisms are crucial for DED treatment. In our study, we observed decreased CMTM6 expression in DED and negatively correlated with the disease severity. Additionally, *Cmtm6*$^{-/-}$ mice exhibited exacerbated DE symptoms, and knockdown of *CMTM6* in HCE-T cells enhanced inflammatory response under hyperosmotic stress. These findings support CMTM6 as a potential therapeutic target for DED treatment.

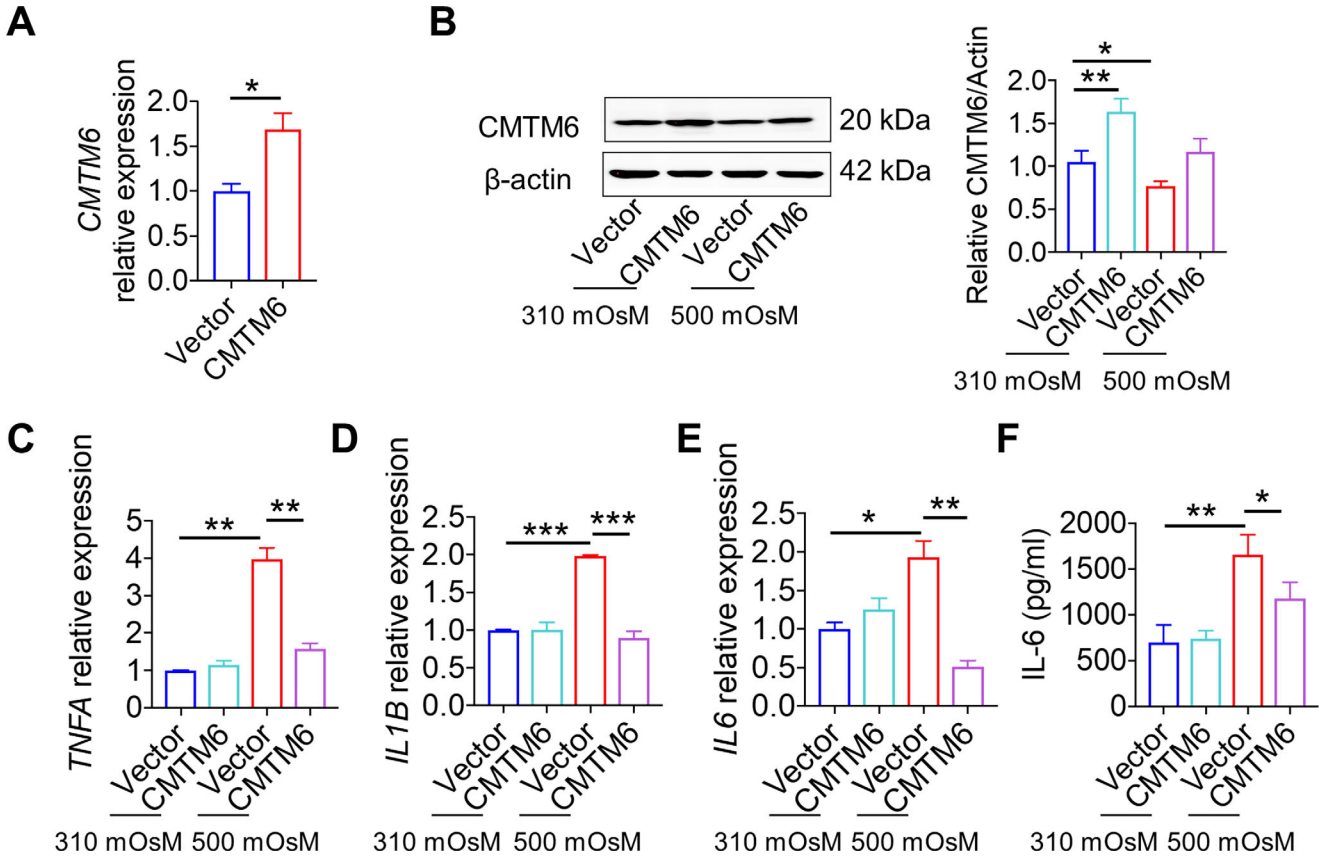

Figure 6. CMTM6 attenuates inflammation stimulated by hyperosmolarity in HCE-T cells. A TG006-CMTM6-IRES-EGFP lentiviral vector was used to overexpress CMTM6. The TG006 lentiviral vector was used as a negative control. (**A**, **B**) Overexpression of CMTM6 in HCE-T cells was validated using RT-PCR (**A**) and western blot analyses (**B**). (**C–E**) RT-PCR was used to detect the mRNA levels of *TNFA* (**C**), *IL1B* (**D**), and *IL6* (**E**). (F) The protein level of IL-6 in the culture supernatant was measured using CBA. Two-group statistical analysis was conducted using the unpaired Student's *t*-test (**A**). Four groups were compared using one-way ANOVA followed by Tukey's multiple comparisons test (**B–F**). $^{*}P < 0.05$, $^{**}P < 0.01$, $^{***}P < 0.001$.

The ocular surface epithelium not only defends against the invasion of microbial and non-microbial pathogens but also faces different physical and environmental challenges.[40] In order to regulate the inflammatory balance of the ocular surface, the corneal epithelium secretes a variety of immune-modulating factors (including NTN-1,[41] PEDF,[17] and TSP-118) to modulate ocular surface inflammation. In DED, PEDF and TSP-1 expression is upregulated and NTN-1 expression is downregulated, suggesting that various immunomodulatory factors participate in DED through distinct mechanisms. Our discovery of decreased CMTM6 expression in corneal and conjunctival epithelial cells in DED indicates that CMTM6 may contribute to the onset and progression of this disease.

DED is a prevalent ocular disorder characterized by inflammation of the ocular surface.[42] Understanding its immune regulatory mechanisms is crucial for unraveling its pathogenesis. Although CMTM6 is a potential novel immunotherapy target for various cancers such as hepatocellular carcinoma,[43] glioma,[44] and neck squamous cell carcinoma,[45] its function in inflammation, including DED, remains unknown. $CD4^+$ T cells, encompassing Th1, Th17, and Tregs, play a central role in the pathogenesis of DED.[1,39] Th1 and Th17 cells are central in driving autoimmune damage in DED.[2,46,47] The elevated Th1 and Th17 cells in the DLNs migrate toward the ocular surface,[48] with Th1 cells primarily secreting IFN-γ, leading to the disruption of conjunctival goblet cells,[49] and Th17 cells secreting IL-17A, directly breaking the corneal epithelial barrier and boosting the generation of inflammatory factors.[50] These processes exacerbate the inflammatory cascade at the ocular surface. In our study, *Cmtm6*$^{-/-}$ DE mice exhibited an increase in the numbers of Th1 and Th17 cells in the DLNs, but the number of Tregs was not significantly different between the two groups. Furthermore, our investigation revealed elevated levels of corneal and tear proinflammatory cytokines in Collectively, these findings strongly indicate that CMTM6 exerts a protective effect against DE by effectively suppressing the inflammatory response. A recent study reported that CMTM6 promotes the stability of CD58, an adhesion molecule that contributes to the initial binding of effector T cells through endosomal recycling.[51] However, the specific regulatory mechanisms by which CMTM6 influences Th1 and Th17 cells in DED warrant further investigations using conditional knockout mice (for example, $CD4^{Cre}$*Cmtm6*$^{fl/fl}$).

Previous research has demonstrated a significant upregulation of PD-L1 in corneal epithelial cells.[52] El Annan et al.[53] reported decreased PD-L1 in DED, and PD-L1 worsened inflammation by upregulating the expression of chemokine receptors that drove more $CD3^+$ T cells to the ocular surface. Considering that CMTM6 stabilizes PD-L1 expression,[24,25] we assessed PD-L1 expression and found it was downregulated after the knockdown of *CMTM6* in HCE-T cells

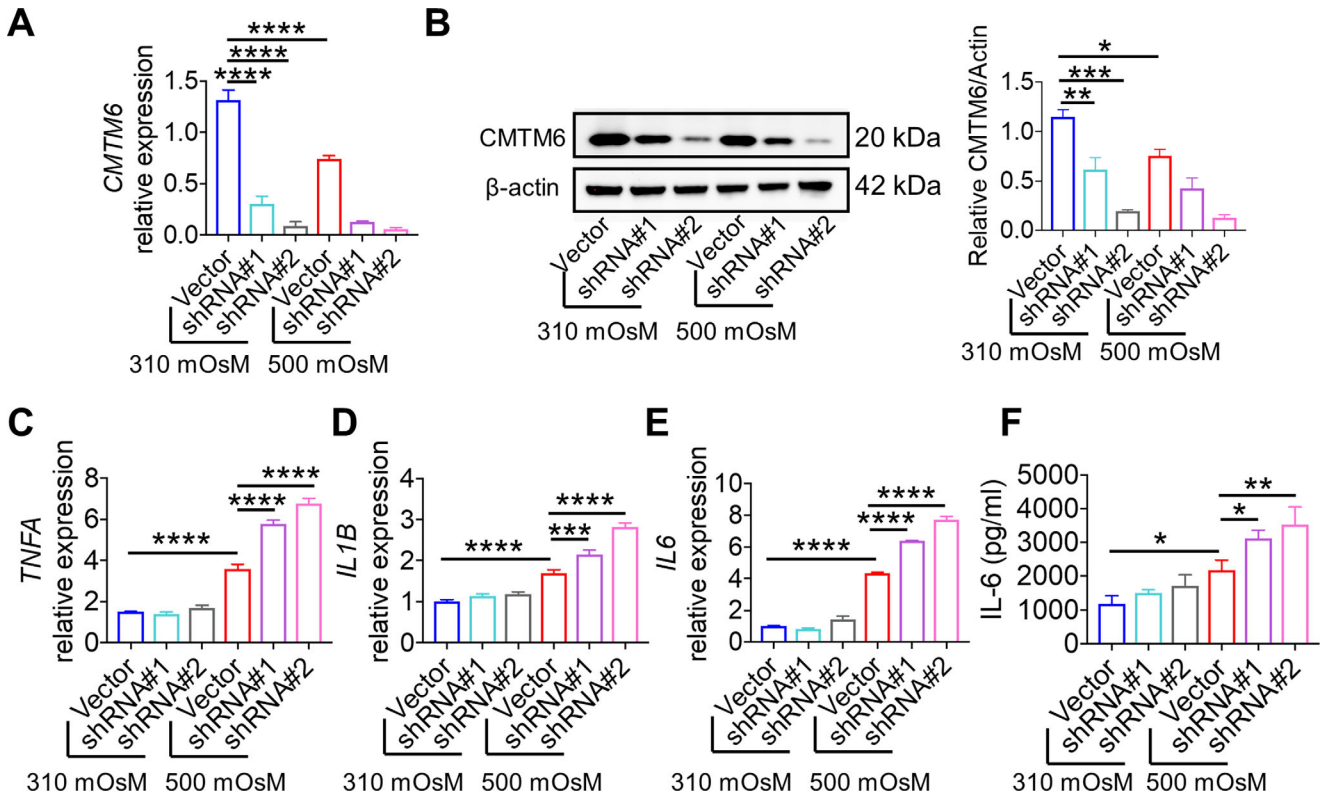

Figure 7. Knockdown of *CMTM6* enhances inflammation stimulated by hyperosmolarity in HCE-T cells. Knockdown of *CMTM6* using shRNA promotes inflammation stimulated by hyperosmolarity in HCE-T cells. A lentivirus encoding a CMTM6 shRNA was used to silence CMTM6 expression. A lentivirus expressing control shRNA (shNC) was used as a negative control. (**A**) RT-PCR was used to detect the mRNA level of CMTM6 in HCE-T cells. (**B**) Western blot analysis was used to examine the protein level of CMTM6 in HCE-T cells. (**C–E**) Cultured cells were collected to assess the mRNA expression of *TNFA* (**C**), *IL1B* (**D**), and *IL6* (**E**). (**F**) IL-6 release was quantified in the culture supernatant using CBA. Six groups were compared using one-way ANOVA followed by Tukey's multiple comparisons test. $^{*}P < 0.05$, $^{**}P < 0.01$, $^{***}P < 0.001$, $^{****}P < 0.0001$.

(data not shown). Therefore, we hypothesized that CMTM6 could exert its effects by modulating PD-L1 expression in DED; however, whether CMTM6 can stabilize PD-L1 in DED remains to be confirmed.

Tight junctions are crucial for maintaining the integrity and function of the corneal barrier. ZO-1 interacts with transmembrane proteins on the cell membrane and effectively anchors them to the actin cytoskeleton, ensuring the closure of intercellular gaps between epithelial cells.[54] The MARVEL structural domain of CMTM6 plays a significant role in vesicle transport and tight intercellular junctions.[55] Our findings suggest that CMTM6 protects the epithelial barrier by acting on ZO-1. Further research is needed to figure out the role of CMTM6 in ZO-1 protein stability. The mechanisms underlying barrier disruption in DED remain elusive. Hyperosmolarity-induced inflammatory mediators can damage tight junction proteins, leading to corneal barrier disruption,[16] and dysfunction or apoptosis of apical corneal epithelial cells may contribute to impairment of the corneal barrier.[56] Additionally, inflammation has been linked to barrier breakdown, although the exact mechanism remains unclear. Whether CMTM6 initially inhibits inflammatory responses or prioritizes barrier protection, or both, merits further investigation.

Previous studies have demonstrated that reduction of CMTM6 in 786-O cells results in the robust upregulation of the expression of numerous inflammatory cytokines, including IL-1β, TNF-α, and IL-6.[57] Furthermore, *CMTM6* knockdown in oral squamous cell carcinoma cells increases expression of the proinflammatory cytokines TNF-α and IL-12p40 in the tumor microenvironment,[58] consistent with our findings. Evidence has shown that the intracellular signaling pathways MAPK and NF-κB perform essential parts in the signal transduction in chronic inflammatory disorders, including DED.[59] Huang et al.[60] reported that CMTM6 activates the MAPK/JNK/p38 signaling pathway, which in turn promotes invasion, migration, and proliferation of cervical cancer cells. In addition, in JIMT-1 tumor cells lacking CMTM6, the expression of HER2, p-HER2, PI3K, and AKT is reduced.[61] However, there have been no reports on the relationship between CMTM6 and NF-κB p65. In this study, we showed, for the first time, to the best of our knowledge, that activation of NF-κB p65 is regulated by CMTM6 in DED and that silencing *CMTM6* had a suppressive effect on proinflammatory cytokines release via downregulating the activation of the NF-κB/p65 signaling pathway. Consistent with previous reports that p65 is strongly associated with inflammation stimulated by hyperosmotic media,[10–12] we observed that inhibition of p65 prominently alleviated the expression of TNF-α, IL-1β, and IL-6, which are aggravated by CMTM6 silencing. Hence, our results strongly suggest that CMTM6 suppresses inflammation by inhibiting the NF-κB p65 signaling pathway.

NF-κB serves as a vital transcription factor activated by various extracellular stimuli through classical or alternative pathways to mediate inflammatory or immune responses.[62] Meanwhile, much attention has been devoted to treating autoimmune diseases by inhibiting NF-κB.[63] An inhibitor of

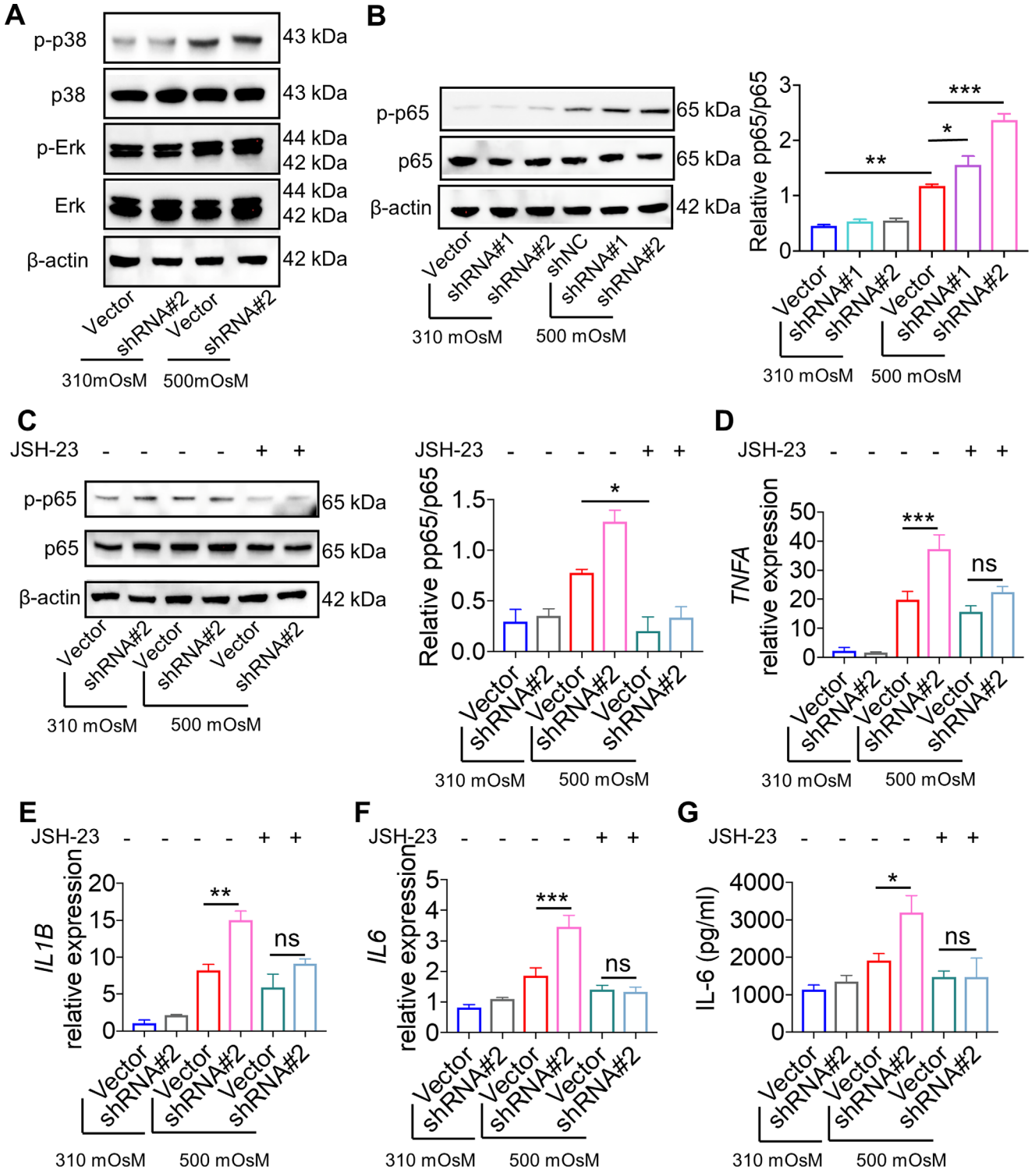

Figure 8. CMTM6 suppresses inflammation through the NF-κB/p65 pathway in HCE-T cells under hyperosmotic stress. (**A**, **B**) The effect of CMTM6 on the activation of p38 (**A**), Erk (**A**), and p65 (**B**) was examined using western blot analysis. (**C–G**) For the treatment of p65 inhibition, 50 µM JSH-23 was added to the cell culture medium, followed by incubation with 500-mOsM media for 8 or 24 hours. DMSO was used as a control. (**C**) The effect of JSH-23 was detected using western blot analysis. (**D–F**) The mRNA levels of *TNFA* (**D**), *IL1B* (**E**), and *IL6* (**F**) were examined using RT-PCR. (**G**) The protein level of IL-6 in cell culture supernatants was detected using CBA. Six groups were compared using one-way ANOVA followed by Tukey's multiple comparisons test. $^{*}P < 0.05$, $^{**}P < 0.01$, $^{***}P < 0.001$.

NF-κB p65 nuclear translocation, referred to as iguratimod, has been approved for the treatment of rheumatoid arthritis.[64] Our study demonstrated the capability of CMTM6 to inhibit NF-κB p65 activation. However, whether CMTM6 can serve as an endogenous anti-inflammatory mediator, modulating the NF-κB pathway for treating DED or other autoimmune diseases, remains to be determined. Additionally, the mechanism by which NF-κB becomes activated by hyperos-

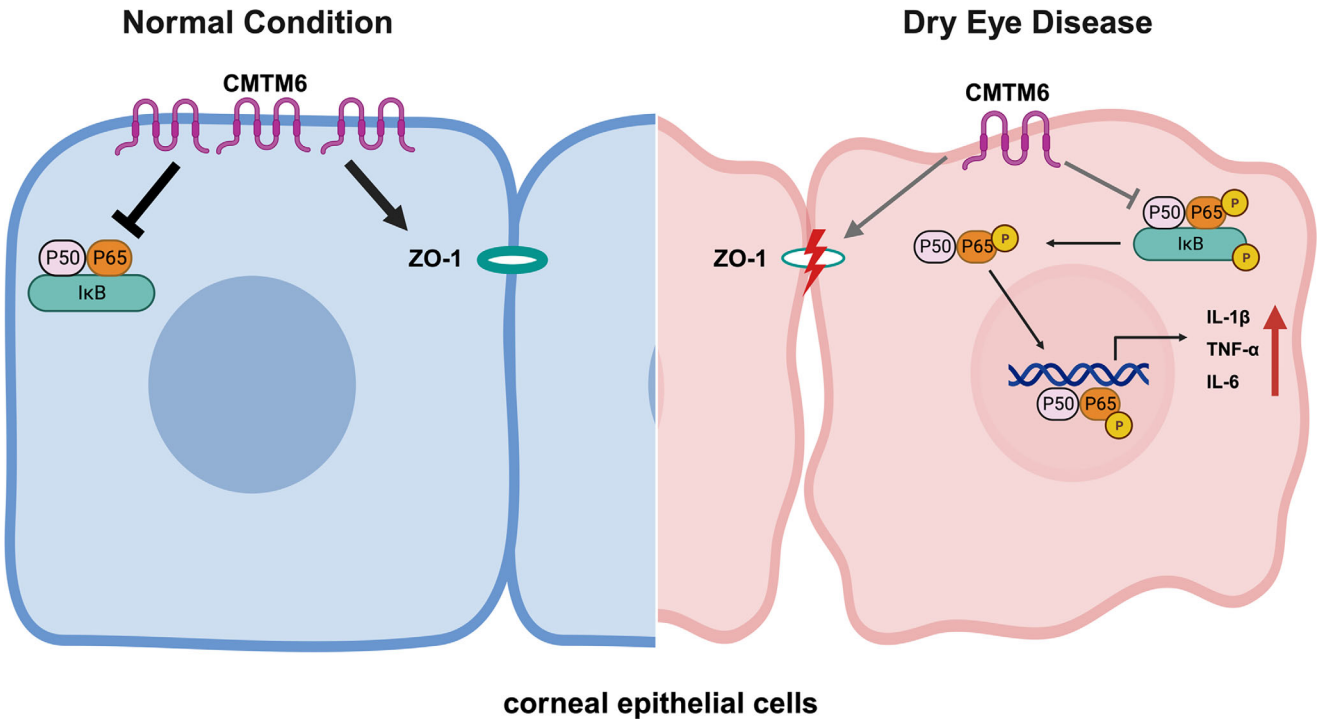

Figure 9. Graph abstract of how CMTM6 regulates inflammatory response and barrier function in the pathogenesis of DED. Under normal conditions, CMTM6 exhibits high expression levels in the corneal epithelium. However, following the onset of dry eye, CMTM6 expression is notably downregulated. CMTM6 plays a pivotal role in preventing corneal epithelial cells from generating an excessive inflammatory response by inhibiting NF-κB p65, thereby mitigating inflammatory response and ameliorating epithelial barrier disruption in DED. Figure was created using BioRender (http://biorender.com/).

motic stimuli in DED remains unclear. Further investigation is necessary to elucidate the interactions between CMTM6 and NF-κB.

In conclusion, this study demonstrated that CMTM6 was decreased in the DED patients, DE mice, and HCE-T cells. CMTM6 inhibits the inflammatory response and improves the corneal epithelial barrier function in this disease (Fig. 9). Our results highlight the pivotal role of NF-κB p65 in mediating CMTM6 in DED and suggest the potential implication of CMTM6–NF-κB p65 signaling as a treatment target for patients with DED.

Acknowledgments

The authors thank the National Natural Science Foundation of China and Beijing Municipal Natural Science Foundation.

Supported by grants from the National Natural Science Foundation of China (82171022, 81974128, and 81971472); Beijing Municipal Natural Science Foundation (7202081); Peking University Medicine Sailing Program for Young Scholars' Scientific & Technological Innovation (BMU2023YFJHPY016); and the China Postdoctoral Science Foundation (2023M730122).

Disclosure: **Y. Zhou**, None; **B. Ma**, None; **Q. Liu**, None; **H. Duan**, None; **Y. Huo**, None; **L. Zhao**, None; **J. Chen**, None; **W. Han**, None; **H. Qi**, None

References

1. Craig JP, Nichols KK, Akpek EK, et al. TFOS DEWS II Definition and Classification Report. *Ocul Surf*. 2017;15(3):276–283.
2. Chen Y, Dana R. Autoimmunity in dry eye disease – an updated review of evidence on effector and memory Th17 cells in disease pathogenicity. *Autoimmun Rev*. 2021;20(11):102933.
3. Stapleton F, Alves M, Bunya VY, et al. TFOS DEWS II Epidemiology Report. *Ocul Surf*. 2017;15(3):334–365.
4. Morthen MK, Magno MS, Utheim TP, Hammond CJ, Vehof J. The work-related burden of dry eye. *Ocul Surf*. 2023;28:30–36.
5. Yang W, Luo Y, Wu S, et al. Estimated annual economic burden of dry eye disease based on a multi-center analysis in China: a retrospective study. *Front Med (Lausanne)*. 2021;8:771352.
6. Jones L, Downie LE, Korb D, et al. TFOS DEWS II Management and Therapy Report. *Ocul Surf*. 2017;15(3):575–628.
7. de Paiva CS, Pflugfelder SC, Ng SM, Akpek EK. Topical cyclosporine A therapy for dry eye syndrome. *Cochrane Database Syst Rev*. 2019;9(9):Cd010051.
8. Yoon CH, Jang HJ, Ryu JS, et al. 1,5-Dicaffeoylquinic acid from *Pseudognaphalium affine* ameliorates dry eye disease via suppression of inflammation and protection of the ocular surface. *Ocul Surf*. 2023;29:469–479.
9. Perez VL, Stern ME, Pflugfelder SC. Inflammatory basis for dry eye disease flares. *Exp Eye Res*. 2020;201:108294.
10. Corrales RM, Stern ME, De Paiva CS, Welch J, Li DQ, Pflugfelder SC. Desiccating stress stimulates expression of matrix metalloproteinases by the corneal epithelium. *Invest Ophthalmol Vis Sci*. 2006;47(8):3293–3302.
11. Luo L, Li DQ, Corrales RM, Pflugfelder SC. Hyperosmolar saline is a proinflammatory stress on the mouse ocular surface. *Eye Contact Lens*. 2005;31(5):186–193.
12. Stern ME, Schaumburg CS, Pflugfelder SC. Dry eye as a mucosal autoimmune disease. *Int Rev Immunol*. 2013;32(1):19–41.

13. Luo L, Li DQ, Doshi A, Farley W, Corrales RM, Pflugfelder SC. Experimental dry eye stimulates production of inflammatory cytokines and MMP-9 and activates MAPK signaling pathways on the ocular surface. *Invest Ophthalmol Vis Sci*. 2004;45(12):4293–4301.
14. Pflugfelder SC, Stern ME. Mucosal environmental sensors in the pathogenesis of dry eye. *Expert Rev Clin Immunol*. 2014;10(9):1137–1140.
15. Hu J, Gao N, Zhang Y, et al. IL-33/ST2/IL-9/IL-9R signaling disrupts ocular surface barrier in allergic inflammation. *Mucosal Immunol*. 2020;13(6):919–930.
16. Leong YY, Tong L. Barrier function in the ocular surface: from conventional paradigms to new opportunities. *Ocul Surf*. 2015;13(2):103–109.
17. Ma B, Zhou Y, Liu R, et al. Pigment epithelium-derived factor (PEDF) plays anti-inflammatory roles in the pathogenesis of dry eye disease. *Ocul Surf*. 2021;20:70–85.
18. Tan X, Chen Y, Foulsham W, et al. The immunoregulatory role of corneal epithelium-derived thrombospondin-1 in dry eye disease. *Ocul Surf*. 2018;16(4):470–477.
19. Zhou Y, Lin J, Peng X, et al. The role of netrin-1 in the mouse cornea during *Aspergillus fumigatus* infection. *Int Immunopharmacol*. 2019;71:372–381.
20. Schleimer RP, Kato A, Kern R, Kuperman D, Avila PC. Epithelium: at the interface of innate and adaptive immune responses. *J Allergy Clin Immunol*. 2007;120(6):1279–1284.
21. Han W, Lou Y, Tang J, et al. Molecular cloning and characterization of chemokine-like factor 1 (CKLF1), a novel human cytokine with unique structure and potential chemotactic activity. *Biochem J*. 2001;357(pt 1):127–135.
22. Han W, Ding P, Xu M, et al. Identification of eight genes encoding chemokine-like factor superfamily members 1–8 (*CKLFSF1–8*) by in silico cloning and experimental validation. *Genomics*. 2003;81(6):609–617.
23. Wu J, Li L, Wu S, Xu B. CMTM family proteins 1–8: roles in cancer biological processes and potential clinical value. *Cancer Biol Med*. 2020;17(3):528–542.
24. Burr ML, Sparbier CE, Chan YC, et al. CMTM6 maintains the expression of PD-L1 and regulates anti-tumour immunity. *Nature*. 2017;549(7670):101–105.
25. Mezzadra R, Sun C, Jae LT, et al. Identification of CMTM6 and CMTM4 as PD-L1 protein regulators. *Nature*. 2017;549(7670):106–110.
26. Knight JS, Meng H, Coit P, et al. Activated signature of antiphospholipid syndrome neutrophils reveals potential therapeutic target. *JCI Insight*. 2017;2(18):e93897.
27. Zeisbrich M, Chevalier N, Sehnert B, et al. CMTM6-deficient monocytes in ANCA-associated vasculitis fail to present the immune checkpoint PD-L1. *Front Immunol*. 2021;12:673912.
28. Chinese expert consensus on the definition and classification of dry eye (2020). *Zhonghua Yan Ke Za Zhi*. 2020;56(6):418–422.
29. Chinese expert consensus on the examination and diagnosis of dry eye (2020). *Zhonghua Yan Ke Za Zhi*. 2020;56(10):741–747.
30. Duan H, Yang T, Zhou Y, et al. Comparison of mucin levels at the ocular surface of visual display terminal users with and without dry eye disease. *BMC Ophthalmol*. 2023;23(1):189.
31. Song XJ, Li DQ, Farley W, et al. Neurturin-deficient mice develop dry eye and keratoconjunctivitis sicca. *Invest Ophthalmol Vis Sci*. 2003;44(10):4223–4229.
32. Li L, Li Y, Zhu X, et al. Conjunctiva resident $\gamma\delta$ T cells expressed high level of IL-17A and promoted the severity of dry eye. *Invest Ophthalmol Vis Sci*. 2022;63(12):13.
33. Chen Y, Pu J, Li X, et al. Aim2 deficiency ameliorates lacrimal gland destruction and corneal epithelium defects in an experimental dry eye model. *Invest Ophthalmol Vis Sci*. 2023;64(3):26.
34. Huang X, Xiang L, Wang B, et al. CMTM6 promotes migration, invasion, and EMT by interacting with and stabilizing vimentin in hepatocellular carcinoma cells. *J Transl Med*. 2021;19(1):120.
35. Lin H, Lin J, Pan T, et al. Polymeric immunoglobulin receptor deficiency exacerbates autoimmune hepatitis by inducing intestinal dysbiosis and barrier dysfunction. *Cell Death Dis*. 2023;14(1):68.
36. Bron AJ, de Paiva CS, Chauhan SK, et al. TFOS DEWS II pathophysiology report. *Ocul Surf*. 2017;15(3):438–510.
37. Yamaguchi T. Inflammatory response in dry eye. *Invest Ophthalmol Vis Sci*. 2018;59(14):Des192–Des199.
38. Li JM, Lu R, Zhang Y, et al. IL-36α/IL-36RA/IL-38 signaling mediates inflammation and barrier disruption in human corneal epithelial cells under hyperosmotic stress. *Ocul Surf*. 2021;22:163–171.
39. Chen Y, Wang S, Alemi H, Dohlman T, Dana R. Immune regulation of the ocular surface. *Exp Eye Res*. 2022;218:109007.
40. Barabino S, Chen Y, Chauhan S, Dana R. Ocular surface immunity: homeostatic mechanisms and their disruption in dry eye disease. *Prog Retin Eye Res*. 2012;31(3):271–285.
41. Yu C, Chen P, Xu J, et al. Corneal epithelium-derived netrin-1 alleviates dry eye disease via regulating dendritic cell activation. *Invest Ophthalmol Vis Sci*. 2022;63(6):1.
42. Dogru M, Kojima T, Simsek C, Tsubota K. Potential role of oxidative stress in ocular surface inflammation and dry eye disease. *Invest Ophthalmol Vis Sci*. 2018;59(14):Des163–Des168.
43. Huang Y, Zhu Y, Yang J, et al. CMTM6 inhibits tumor growth and reverses chemoresistance by preventing ubiquitination of p21 in hepatocellular carcinoma. *Cell Death Dis*. 2022;13(3):251.
44. Wei L, Wei Q, Yang X, Zhou P. CMTM6 knockdown prevents glioma progression by inactivating the mTOR pathway. *Ann Transl Med*. 2022;10(4):181.
45. Chen L, Yang QC, Li YC, et al. Targeting CMTM6 suppresses stem cell-like properties and enhances antitumor immunity in head and neck squamous cell carcinoma. *Cancer Immunol Res*. 2020;8(2):179–191.
46. De Paiva CS, Chotikavanich S, Pangelinan SB, et al. IL-17 disrupts corneal barrier following desiccating stress. *Mucosal Immunol*. 2009;2(3):243–253.
47. Chauhan SK, El Annan J, Ecoiffier T, et al. Autoimmunity in dry eye is due to resistance of Th17 to Treg suppression. *J Immunol*. 2009;182(3):1247–1252.
48. Pflugfelder SC, Corrales RM, de Paiva CS. T helper cytokines in dry eye disease. *Exp Eye Res*. 2013;117:118–125.
49. Bian F, Xiao Y, Barbosa FL, et al. Age-associated antigen-presenting cell alterations promote dry-eye inducing Th1 cells. *Mucosal Immunol*. 2019;12(4):897–908.
50. Chen Y, Shao C, Fan NW, et al. The functions of IL-23 and IL-2 on driving autoimmune effector T-helper 17 cells into the memory pool in dry eye disease. *Mucosal Immunol*. 2021;14(1):177–186.
51. Ho P, Melms JC, Rogava M, et al. The CD58-CD2 axis is co-regulated with PD-L1 via CMTM6 and shapes anti-tumor immunity. *Cancer Cell*. 2023;41(7):1207–1221.e12.
52. Shen L, Jin Y, Freeman GJ, Sharpe AH, Dana MR. The function of donor versus recipient programmed death-ligand 1 in corneal allograft survival. *J Immunol*. 2007;179(6):3672–3679.
53. El Annan J, Goyal S, Zhang Q, Freeman GJ, Sharpe AH, Dana R. Regulation of T-cell chemotaxis by programmed death-ligand 1 (PD-L1) in dry eye-associated corneal inflammation. *Invest Ophthalmol Vis Sci*. 2010;51(7):3418–3423.

Investigative Ophthalmology & Visual Science

54. Belardi B, Hamkins-Indik T, Harris AR, Kim J, Xu K, Fletcher DA. A weak link with actin organizes tight junctions to control epithelial permeability. *Dev Cell*. 2020;54(6):792–804.e7.
55. Sánchez-Pulido L, Martín-Belmonte F, Valencia A, Alonso MA. MARVEL: a conserved domain involved in membrane apposition events. *Trends Biochem Sci*. 2002;27(12):599–601.
56. Beardsley RM, De Paiva CS, Power DF, Pflugfelder SC. Desiccating stress decreases apical corneal epithelial cell size–modulation by the metalloproteinase inhibitor doxycycline. *Cornea*. 2008;27(8):935–940.
57. Wang H, Fan Y, Chen W, et al. Loss of CMTM6 promotes DNA damage-induced cellular senescence and antitumor immunity. *Oncoimmunology*. 2022;11(1):2011673.
58. Pang X, Wang SS, Zhang M, et al. OSCC cell-secreted exosomal CMTM6 induced M2-like macrophages polarization via ERK1/2 signaling pathway. *Cancer Immunol Immunother*. 2021;70(4):1015–1029.
59. Ling J, Chan CL, Ho CY, et al. The extracts of dendrobium alleviate dry eye disease in rat model by regulating aquaporin expression and MAPKs/NF-κB Signalling. *Int J Mol Sci*. 2022;23(19):11195.
60. Huang X, Liu W, Liu C, et al. CMTM6 as a candidate risk gene for cervical cancer: comprehensive bioinformatics study. *Front Mol Biosci*. 2022;9:983410.
61. Xing F, Gao H, Chen G, et al. CMTM6 overexpression confers trastuzumab resistance in HER2-positive breast cancer. *Mol Cancer*. 2023;22(1):6.
62. Zhang Q, Lenardo MJ, Baltimore D. 30 years of NF-κB: a blossoming of relevance to human pathobiology. *Cell*. 2017;168(1–2):37–57.
63. Ramadass V, Vaiyapuri T, Tergaonkar V. Small molecule NF-κB pathway inhibitors in clinic. *Int J Mol Sci*. 2020;21(14):5164.
64. Tanaka K, Yamaguchi T, Hara M. Iguratimod for the treatment of rheumatoid arthritis in Japan. *Expert Rev Clin Immunol*. 2015;11(5):565–573.

Investigative Ophthalmology & Visual Science